Korean J. Chem. Eng., 33(2), 587-593 (2016)
DOI: 10.1007/s11814-015-0152-5

pISSN: 0256-1115
eISSN: 1975-7220

CO_2 fixation and lipid production by microalgal species

Pavani Parupudi*, Chandrika Kethineni*, Pradip Babanrao Dhamole, Sandeep Vemula*, Prasada Rao Allu***, Mahendran Botlagunta*, Sujana Kokilagadda*, and Srinivasa Reddy Ronda*,†**

*Department of Biotechnology, KLEF University, Vaddeswaram-522 502, Guntur, AP, India
**Department of Chemical Engineering, Visvesvaraya National Institute of Technology, Nagpur, Maharashtra, India
***Department of Horticulture, Sikkim University, Gangtok, Sikkim, India
(*Received 10 February 2015 • accepted 10 July 2015*)

Abstract−Microalgal species *Nannochloropsis limnetica*, *Botryococcus braunii*, and *Stichococcus bacillaris* were compared for their ability to grow, remove CO_2, and accumulate lipids in their biomass under CO_2-enriched atmosphere. Overall, *N. limnetica* outperformed the other two cultures and distinctly exhibited higher specific growth rate (0.999 d^{-1}) and CO_2 fixation rate (0.129 gL^{-1} d^{-1}) with a high specific lipid yield (40% w/w). The volumetric CO_2 fixation rate for all three species was validated with biomass productivity and mass transfer methods (P<0.005 and R^2=0. 98). At 10% CO_2, *N. limnetica* showed one-and-a-half times more carbon fixation efficiency over *B. braunii*, and *S. bacillaris*. On the other hand, total fatty acids of *N. limnetica* dispalyed an apparent increase in oleic acid. Whereas, under similar conditions, *N. limnetica* exhibited reduced eicosapentaenoic acid. These findings suggest that at high CO_2 conditions, *N. limnetica* proved to be an efficient CO_2 capture algal system and can be considered for biofuel applications.

Keywords: Microalgae, Lipid, Biofuel, CO_2 Fixation Rate, Fatty Acid

INTRODUCTION

The study of microalgae has seen a major influx of interest in recent years owing to their ability to fix large amounts of carbon dioxide (CO_2) by photosynthesis and accumulate lipid in the biomass [1]. Next to plants, third-generation biofuel production from microalgae has become a promising source of oil [2] and high value products [3]. Besides CO_2 sequestration, some freshwater and marine microalgal species accumulate lipid up to 70% (w/w dry biomass) [4]. Previous studies reveal moderate to high lipid production in green chlorophytes, such as *Nannochloropsis limnetica* [5], *Bortyococcus braunii* [6], *Stichococcus bacillaris* [7], *Dunaliella salina* [8] and *Phaeodactylum tricornutum* [9].

The biomass and lipid productivity for *B. braunii* with 10% CO_2 at ambient air was 26.55 and 5.51 mg L^{-1} d^{-1}. Also, the lipid productivity was found to increase (3.7-fold) with a shift in CO_2 from 10% to flue gas [10]. To address the slow growth rate effects of *B. braunii* Cheng et al. [6] designed attached cultivation with light dilution using a multi-layer arrayed photobioreactor and reported a biomass productivity of 61 g m^{-2} d^{-1}. However, in a single layered system, at day 10, the biomass, lipid and hydrocarbon productivities were shown to be 5.5, 2.34 and 1.06 g m^{-2} d^{-1}, respectively.

The literature on *Nannochloropsis limnetica* is limited. Nevertheless, in a study with *Nannochloropsis oculata*, Chiu et al. [11] demonstrated a biomass and lipid productivity of 0.441 and 0.113 g L^{-1} d^{-1} at 5% CO_2 while at 10% CO_2 it was shown to be 0.398 and 0.097 g L^{-1} d^{-1} in a semi continuous system. However, they further concluded from growth studies that 2% CO_2 in a semicontinuous system with one-day replacement is beneficial for long-term biomass and lipid yield.

In *Stichiococcus bacillaris* [12], the effect of different CO_2 concentrations (5% and 10%) and pH showed least differences in the biomass and lipid productivities. However, at pH 7, *S. bacillaris* exhibited maximum biomass productivity in laboratory scale photobioreactors. Oliveri et al. [13] studied the effect of photobioreactor design and the operating conditions on *Stichiococcus bacillaris*. They made a comparative study between an inclined bubble column photobioreactor (IBC) and a vertical bubble column photobioreactor (VBC) operated under similar conditions and concluded that, IBC exhibited higher performance than VBC. The study further confirmed that at 5% CO_2, IBC demonstrated relatively higher biomass productivity than VBC.

Previous studies [14-16] related to large scale production of microalgal systems primarily focused on the growth and CO_2 fixation kinetics. However, the quantification of fixed CO_2 is largely based on indirect methods such as the one derived from the biomass productivity [17,18]. Hence, experimental elucidation of the fixed CO_2 by microalgae will furnish more insights in terms of delivery, solubility and fixation of CO_2 at various concentrations by the aqueous suspensions of microalgae grown in a photobioreactor.

Besides growth and development of algal species of specific interest under controlled environment, studies on microalgal lipids, their fatty acid profile and composition play a vital role in production and characterization of biofuels. This includes structural features of the fatty acids such as the chain length, degree of unsaturation and branching of the chain that influence the physical and chemical properties of algal derived biofuels [19]. Studies substantially disclose that high concentrations of CO_2 (supplemented to algae)

†To whom correspondence should be addressed.
E-mail: rsr@kluniversity.in

have a significant effect on the structural features of the fatty acid [20,21]. Whereas, an apparent increase in CO_2 from 0.03 to 2% also reported to increase saturated fatty acids [22].

In contrast, an increase in CO_2 concentrations from 2-5% and 5-20% in *Dunaliella salina* and *Thalassiosira weissflogii* significantly supressed the fatty acid content [23,24]. Yet, restricted information is available on the effect of CO_2 on algal fatty acids; it is interesting to understand the effect of CO_2 on fatty acid fluctuation patterns and subsequently design suitable supplementation strategies for microalgal cultivation leading to biofuel production.

In view of global warming due to elevated CO_2 levels, there is an urgency to explore better acclimatizing microalgal species under high CO_2 concentrations with optimum biomass and lipid productivity. A complete understanding of potential microalgal species with CO_2 transfer methodology helps in production of biofuel for future requirements.

Limited information is available on CO_2 fixation rate, efficiency and the effect of CO_2 on fatty acid profile on *N. limnetica*. Therefore, in the present study, a major emphasis has been placed on characterization of *N. limnetica* (Nl), under different CO_2 concentrations (0.03% to 10%) in comparision with other microalgae: *B. braunii* (Bb) and *S. bacillaris* (Sb). The influence of CO_2 concentration on the growth, specific lipid yield, and CO_2 removal efficiency of all the three strains was investigated. In view of the emphasis on CO_2 fixation and its transfer in the algal culture medium, this work validates the CO_2 fixation rate of the microalgal strains with experimental evidence. The selected microalgal strain was further tested for understanding the role of CO_2 concentration on the fatty acid profile.

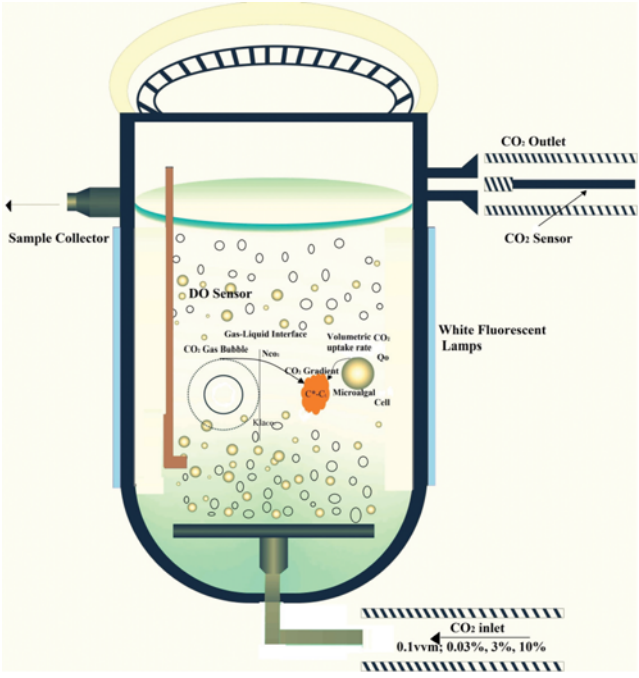

Fig. 1. Schematic illustration of bubble column reactor adapted for CO_2 fixation studies. The reactor design was used for experimental determination of CO_2 transfer rate. The illustration depicts the steady state between the incoming mass of CO_2 transferred (N_{CO_2}) in the bulk liquid and the gradient (C^*-C_L) created by the organism based on its volumentric CO_2 uptake rate (Q_O).

MATERIALS AND METHODS

1. Microalgae and Culture Conditions

Nannochloropsis limnetica 18.99 (Nl), *Botryococcus braunii* 807-1 (Bb), and *Stichococcus bacillaris* 379-1c (Sb) were obtained from the culture collection of algae at Goettingen, SAG, Germany. A series of batch experiments were conducted in a bubble column bioreactor with a working volume of 30 L (Fig. 1). Cool white fluorescent lamps with a light intensity of 100 μmolquanta m^{-2} s^{-1} were mounted on either side of the reactor. In all experiments, the initial cell density was maintained at 0.01 g L^{-1}. Chu 13 medium [25] and Bolds basal medium [12] were used for *B. braunii* and *S. bacillaris* respectively, whereas, *N. limnetica* was grown in Basal medium [26].

Cultures were grown at 30 °C and pH 8.0. Culture conditions were maintained by continuously sparging air comprising 3% and 10% (v/v) CO_2 at 0.1 vvm for eight hours per day. For control, ambient air with 0.03% CO_2 was sparged continuously throughout the day. The oxygen concentration was measured in the reactor using a dissolved oxygen (DO) probe (Oakton DO110,USA), and the inlet and outlet CO_2 concentrations were monitored with a CO_2 sensor (Testo 350-S/-XL, USA).

2. Cell Concentration and Specific Growth Rate

Cell concentration was estimated by using dry weight method (as g L^{-1}, DCW). Triplicate samples (10 mL) were filtered through a constant vacuum (0.44 bar) over pre-weighed and dried Whatman GF/F glass fiber filters (Ø 55 mm, pore size 0.7 μm). The filter with biomass was dried at 105 °C for 3 h in an oven and weighed after cooling at room temperature [27]. The dry weight was noted from the tare weight of the sample. The maximum specific growth rate (μ_{max}) was calculated by using the formula $\ln(X_2-X_1)/\Delta t$, where X_1 and X_2 are the initial and final cell concentrations of the sample, respectively. Δt is the cultivation time in days [28].

3. Harvesting Method and Biomass Productivity

Algal culture was allowed to grow until the stationary phase for maximum cell concentration (X_{max}). Alum($KAl(SO_4)_2 \cdot 12H_2O$) was added (200 mgL^{-1}) as a flocculent for harvesting the batches. The concentrated biomass slurry was dried and recovered as flakes and subsequently powdered, weighed, and stored in a desiccator for analysis. The initial cell concentration was designated as X_o, with X_{max} as the maximum cell concentration. The cell growth (ΔX) during cultivation time Δt was calculated as $\Delta X=X_{max}-X_o$. The biomass productivity (P_x) was calculated using the following equation:

$$P_x = \frac{\Delta X}{\Delta t} \quad (1)$$

where ΔX is the variation of cell concentration (g L^{-1}), Δt is the cultivation time.

4. Total Lipid and Lipid Productivity

Total lipid content was estimated by Folch method [29] based on the extraction of lipids using a 3 : 1 (v/v) mixture of chloroform : methanol. In phase separation, the total lipids were extracted in the lower chloroform phase, and the non-lipid components were

dissolved in the upper methanol layers. The chloroform layer was carefully extracted, centrifuged, de-pigmented, and evaporated for gravimetric analysis. The specific lipid yield ($Y_{p/x}$) was expressed as the weight of lipid per unit weight of dry biomass. The lipid productivity (P_L) was calculated with the following equation:

$$P_L=\Delta P/\Delta t \quad (2)$$

Where, ΔP is the variation of lipid (mg L^{-1}), and Δt is the cultivation time.

5. Total Fatty Acid Estimation

Fatty acids were identified as their esters through the direct transesterification method originally proposed by Lepage and Roy [30]. Dried algal biomass (100 mg) was dissolved in 10 mL of methanol-acetyl chloride at 95 : 5 (v/v) in an airtight glass vial. The mixture was heat-digested at 80 °C for 1 h in a water bath. The methylated esters were re-extracted into n-hexane and concentrated to 1 mL.

Total fatty acids were estimated by gas chromatography (Thermo Scientific 8610) with a flame ionizing detector. A fused silica capillary column with a cyanopropyl polysiloxane stationary phase equivalent to 70% cyanopropyl (SGE, BPX-70, 25 m length x 0.32 mm ID x0.25 μm film thickness) was employed for the detection of fatty acid methyl ester (FAME). The injection and detector ports were maintained at 240 °C and 250 °C, respectively.

Fatty acid analysis involved injecting 0.5 μL of the sample in split mode (1 : 50) with nitrogen as a carrier gas. The following temperature program was adopted for detection of FAME: initial temperature 100 °C, 1 min hold; ramp at 10 °C min^{-1} until 180 °C with 1 min hold; ramp at 10 °C min^{-1} until 240 °C, with a 2 min hold.

6. CO_2 Transfer Rate

6-1. The CO_2 Balance Method

The gas phase CO_2 transfer rate ($NA_{(gas)}$) from gas to liquid was determined by balancing the reactor inlet and outlet molar volumetric flow rates of the gas. Thus,

$$NA(gas)=((F_gP_{AG}/T)_i-(F_gP_{AG}/T)_o)\times M\times N\times 60)/RV_L \quad (3)$$

The CO_2 transfer rate in aqueous form was calculated using the following equation:

$$NA_{(aq)}=NA_{(gas)}\cdot H \quad (4)$$

where, H is Henry's constant for CO_2, R is the universal gas constant (L atm $gmol^{-1}$ K^{-1}), V_L is the total volume of the liquid (L), F_g is the volumetric flow rate (L min^{-1}), P_{AG} is the partial pressure of CO_2 in the gas stream, i and o are the inlet and outlet gas streams, and T is the absolute temperature (K). M is the molecular weight of CO_2 in g $mole^{-1}$ and N is the number of sparging hours in day.

6-2. The Mass Transfer Coefficient Method

The rate of the mass transfer of CO_2 from the gas into the liquid was estimated by using the following equation:

$$N_{CO_2}=kla_{CO_2}(C^*-C_L) \quad (5)$$

where, C^* is the CO_2 concentration in the liquid media in equilibrium with the gas phase, which is the maximum possible concentration of CO_2 at the defined partial pressure (g L^{-1}); C_L is the CO_2 concentration in the liquid media during the exponential phase (g L^{-1}), and $K_{la_{CO_2}}$ (s^{-1}) is the volumetric mass transfer coefficient of CO_2. Also, the maximum solubility of CO_2 is given as:

$$C^*=P\cdot y/H \quad (6)$$

where P is the total gas pressure (atm), y is the mole fraction of CO_2 in the inlet stream, and H is Henry's content for CO_2.

kla_{CO_2} was estimated indirectly by finding an experimental kla_{O_2} by using the static method [31] based on the diffusivity of CO_2 and O_2. Hence,

$$kla_{CO_2}=kla_{O_2}\sqrt{\frac{D_{CO_2}}{D_{O_2}}} \quad (7)$$

where, D_{CO_2} and D_{O_2} are the diffusivities of CO_2 and O_2, respectively.

7. Estimation of Volumetric CO_2 Uptake Rate

The volumetric CO_2 uptake rate (Q_O for the respective algal cultures was calculated by finding the rate of change in the average concentration of the aqueous CO_2 in the exponential growth phase of the algae:

$$\frac{dCL}{dt}=N_{(CO_2)}-Q_O \quad (8)$$

where, dCL/dt is the rate of change in average CO_2 (aq) in the bulk liquid of the reactor. In other words dCL/dt is the net change in molar concentrations of aqueous CO_2 in the bulk liquid with respect to time. The gradient created by the organism is compensated by the incoming gas phase CO_2 flux. Hence, the apparent concentration gradient (dCL/dt) developed at any point of time during the exponential phase is negligible and tends to be zero (dCL/dt=0). Therefore, the volumetric CO_2 uptake rate (Q_O) is always observed equivalent to the mass transfer of CO_2 against the concentration gradient in the bulk liquid of the reactor.

8. Estimation of CO_2 Fixation Rate

The CO_2 fixation rate F_{CO_2} (g L^{-1} d^{-1}) was determined from the overall biomass productivity of the cultures (P_x) according to:

$$F_{CO_2}=\frac{P_x\times 0.5}{M_c}\times M_{CO_2} \quad (9)$$

where, M_c and M_{CO_2} are the molecular weights of carbon and CO_2, respectively, and 50% represents the carbon content of the microalgal biomass.

9. Determination of CO_2 Fixing Efficiency

The CO_2 fixing efficiency (E_{CO_2}) was determined considering the fraction of CO_2 fixation rate to that of the total CO_2 transfer to the bulk liquid in the reactor. Thus, the carbon fixing efficiency was derived from:

$$E_{CO_2}(\%)=\frac{F_{CO_2}}{NA(T)}\times 100 \quad (10)$$

where, NA(T) is the total CO_2 transferred into the system. The total CO_2 transferred in the system can be modeled as:

$$NA_{(T)}=\frac{F_g\cdot P\cdot y_i}{R\cdot V\cdot T}=Qo+\frac{F_g\cdot P\cdot y_o}{R\cdot V\cdot T} \quad (11)$$

where Q_O is volumetric CO_2 uptake rate, F_g is the volumetric gas flow rate (L min^{-1}), P is the total gas pressure (atm), y_i and y_o are the mole fraction of carbon dioxide in the inlet and outlet gas phase,

R is the universal gas constant (0.0821 L atm $gmol^{-1}$ K^{-1}), V is the total volume of the reactor (L), and T is the absolute temperature (K).

10. Statistical Analysis

Statistical analyses were conducted using Graph Pad, InStat 3.0. One-way ANOVA was performed for determination of probability (p) and regression values between groups. The results for growth and lipid parameters were represented as the standard deviation of their mean values. All experiments were repeated in triplicate and the results were reported as the mean value of triplicate samples.

RESULTS AND DISCUSSION

1. Microalgal Screening for Growth-Lipid Production and CO_2 Removal

In *N. limnetica* 18.99 (Nl), *B. braunii* 807-1 (Bb), and *S. bacillaris* 379-1c (Sb), the parameters of growth (X_{max}, P_x and μ_{max}), lipid production ($Y_{p/x}$, P_L), and volumetric CO_2 uptake rate (Q_O) were measured with 3% and 10% CO_2 in ambient air along with the control in various experiments. The study was designed to determine the better acclimatizing species in CO_2-enriched gas for CO_2 removal and lipid production.

1-1. Growth Kinetic Studies

Growth-related parameters (Table 1) are shown for CO_2 concentrations of 0.03%, 3%, and 10% (v/v). The maximum growth rate of 0.999 d^{-1} was observed with Nl, followed by Bb (0.949 d^{-1}) and Sb (0.859 d^{-1}) in 3% CO_2. However, a decreasing trend of growth rate was apparent in 10% CO_2 for all cultures tested in the present study.

A maximum biomass productivity (P_x) of 71.67 mg L^{-1} d^{-1} , 66 mg L^{-1} d^{-1} and 50 mg L^{-1} d^{-1} were recorded for Nl , Bb and Sb, respectively, at 3% CO_2. However, the three strains tested in the present study showed a stable average biomass productivity with shift in CO_2 from 3 to 10%. This trend is more relevant to explaining the CO_2-tolerance of these algal strains. Interestingly, the Bb biomass productivity (64.0 mg L^{-1} d^{-1}) at 10% CO_2 reported earlier [32] is close to that calculated at 3% CO_2 in the present work. On the other hand, the growth kinetic information on Nl is limited. However, growth of *N. oculata* in 10% CO_2 was found to be 25 mg L^{-1} d^{-1} [11], and the growth of Sb reported as 37 mg L^{-1} d^{-1} at 15% CO_2 [12].

1-2. Lipid Accumulation

Lipid accumulation studies (Table 2) revealed a maximum specific lipid yield (Yp/x) of 40% (w/w) in Nl at 10% CO_2. Moreover, all three cultures showed improved specific lipid content with a shift in CO_2 from 0.03% (v/v) to 10% (v/v). The specific yield of lipid in Nl culture was enhanced over control by 4% (w/w) and 10% (w/w) in 3% and 10% CO_2, respectively. However, in 10% CO_2, Bb and Sb showed 32% and 30% (w/w) lipid content, respectively. Overall, the yield shown by Nl found to be highest (40%).

Based on P_x and $Y_{p/x}$, the lipid production rates (P_L) in Nl cultures were recorded as 24.48 mg L^{-1} d^{-1} and 28.0 mg L^{-1} d^{-1} at 3% and 10% CO_2, respectively. In general, high lipid production is accomplished in a balanced growth when P_x and $Y_{p/x}$ are at their maximum. High lipid content was observed in all three cultures grown in stress-free environments. However, under stressed conditions, it is possible to attain high lipid production (w/v) by compensation of lower $Y_{p/x}$ with high P_X, and vice versa. Due to its stable biomass productivity and increased specific lipid content at various CO_2 concentrations (3% and 10%), Nl had higher lipid productivity than other cultures.

The specific lipid content reported in the earlier works with Bb [33] was 22% (w/w), while that of Sb [12] reported was 34% and 27% (w/w) at 5% and 15% CO_2, respectively. The fatty acid content in Nl biomass reported by Krienitz et al. [34] was 351 μg mg^{-1} of carbon in the biomass. However, the result could not be compared with the present data since the fatty acid content measurement in earlier work was based on carbon content in the biomass.

1-3. CO_2 Fixation Studies and the Efficiency of CO_2 Removal

The volumetric CO_2 uptake rate (Q_O) shown in Eq. (8) is both a system-driven and organism-dependent parameter. In the context of organism selection based on the CO_2 fixation rate (F_{CO_2}) and

Table 1. Maximum cell concentration (X_{max}), biomass productivity (P_x) and maximum specific growth rate (μ_{max}) of *N. limnetica*, *B. braunii*, and *S. bacillaris* under different CO_2 concentrations. The data at each CO_2 treatment represent mean±SD value of triplicate samples drawn from three repeated experiments

CO_2 (%)	X_{max} (g L^{-1})			P_x (mg L^{-1} d^{-1})			μ_{max} (d^{-1})		
	Nl	Bb	Sb	Nl	Bb	Sb	Nl	Bb	Sb
0.03	0.22±0.02	0.16±0.01	0.15±0.02	17.0±0.5	15.6±0.1	15.2±0.2	0.626±0.003	0.792±0.004	0.763±0.005
3	0.50±0.02	0.34±0.02	0.30±0.03	71.7±0.2	66.0±0.5	50.0±0.4	0.999±0.001	0.949±0.003	0.859±0.002
10	0.35±0.03	0.22±0.04	0.19±0.06	70.0±0.3	60.0±0.3	47.5±0.1	0.829±0.002	0.726±0.004	0.630±0.004

Table 2. Lipid yield and productivity of *N. limnetica*, *B. braunii*, and *S. bacillaris* grown under different CO_2 concentrations. The data at each CO_2 treatment represent mean±SD value of triplicate samples drawn from three repeated experiments

CO_2 (%)	Y_{px} (g g^{-1})			P_L (mg L^{-1} d^{-1})		
	Nl	Bb	Sb	Nl	Bb	Sb
0.03	0.30±0.01	0.23±0.03	0.24±0.02	5.10±0.03	3.58±0.02	3.65±0.02
3	0.34±0.02	0.28±0.02	0.26±0.03	24.48±0.02	18.48±0.03	13.00±0.04
10	0.40±0.03	0.32±0.02	0.30±0.03	28.00±0.03	19.20±0.02	14.25±0.01

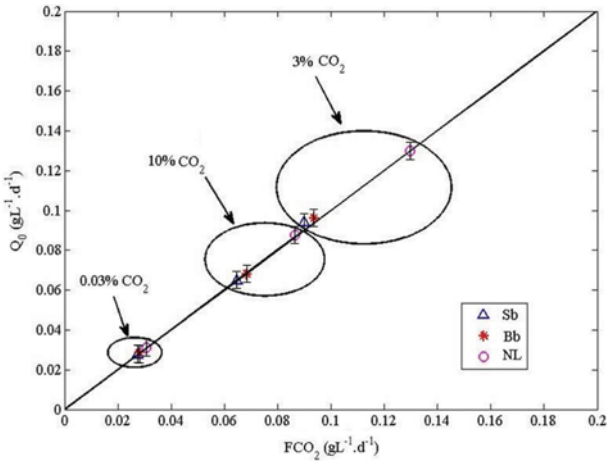

Fig. 2. Validation plot between CO_2 fixation rate (F_{CO_2}) and volumetric CO_2 uptake rate (Q_O) for various algal species under the study. F_{CO_2} being a theoretical parameter, was extrapolated against the experimental CO_2 uptake rate. Data on the line of fit shows that both parameters equally quantify CO_2 fixation rate. The data points represented at each CO_2 concentration are mean values of triplicate samples drawn from three repeated experiments (statistical significance; one-way ANOVA; Between the groups $p<0.001$ and $r^2=0.98$).

efficiency, the reactor design being constant, the CO_2 gradient created by the alga plays a key role in determining a better Q_O for each organism. In this work, F_{CO_2}, a theoretical fixation rate, is correlated with experimental Q_O. The regression of the data (Fig. 2) between Q_O *vs.* F_{CO_2} for all organisms (data points) are well correlated with $p<0.001$ and $r^2=0.98$. Thus, the data on line of fit validate the CO_2 fixation used in the calculation of CO_2 fixing efficiency.

In the present work (Table 3), higher lipid production in Nl had an F_{CO_2} that was 2.52 times (on an average) higher at 3% CO_2 and 2.64 times higher at 10% CO_2 than those of Bb and Sb. However, the CO_2 fixation rate was found to be consistent (0.12 g L^{-1} d^{-1}) at 3% and 10% CO_2 for Nl. The CO_2 fixing efficiency (E_{CO_2}) measures the index of the CO_2 fixation rate and total CO_2 transfer rate in the system. Hence, validation of Q_O or its equivalent parameter F_{CO_2} is essential to establish the accuracy of the data considered for calculation of E_{CO_2}. In this work, validation of the data for Q_O is performed in two stages; the first evidence comes from Q_O *vs* P_x plot (Fig. 3(a)), wherein the correlation between two parameters is proven to be 1.8 times the P_x. Earlier work also reported a similar correlation between CO_2 fixation and P_x [18,35]. Validation of Q_O and P_x (Fig. 3(a)) reconfirms the stoichiometric relation between these parameters. In the second stage of validation of Q_O, two independent experiments were carried to evaluate the accuracy of Q_O

Table 3. CO_2 fixation rate (F_{CO_2}) and effeciency of *N. limnetica*, *B. braunii* and *S. bacillaris* grown under various CO_2 concentrations. The data at each CO_2 treatment represent mean±SD value of triplicate samples drawn from three repeated experiments

CO_2 (%)	F_{CO_2} (g L^{-1} d^{-1})			E_{CO_2}%		
	Nl	Bb	Sb	Nl	Bb	Sb
0.03	0.031±0.020	0.028±0.015	0.027±0.020	81.64	74.91	73.00
3	0.129±0.012	0.118±0.013	0.090±0.015	13.35	11.97	10.71
10	0.126±0.015	0.108±0.002	0.086±0.012	8.26	6.13	5.00

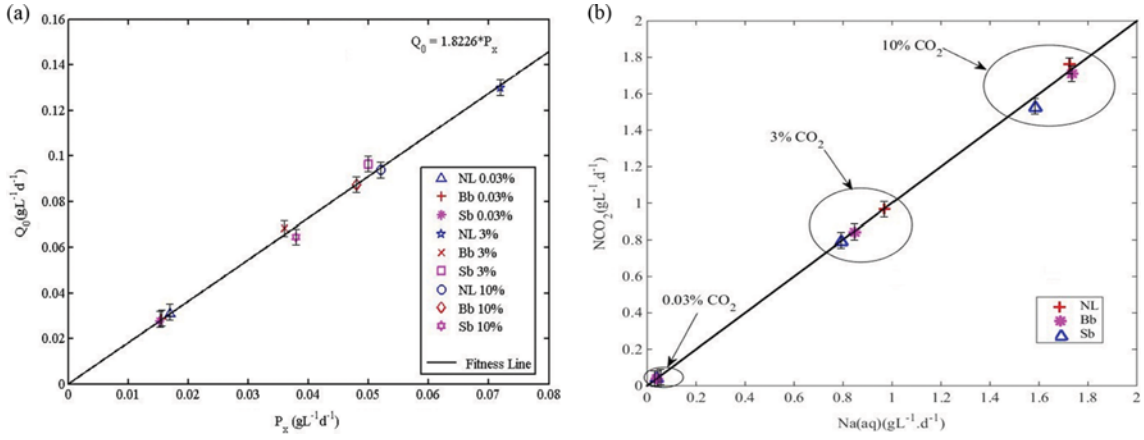

Fig. 3. (a) Validation of CO_2 fixation rate with biomass productivity. A correlation of CO_2 fixation data with respect to the biomass productivity for three algae was tested at various CO_2 concentrations. The data point with a constant slope shows that the carbon content and the biomass quantity follow a stoichiometric relation with sequestered CO_2 being 1.8 times the biomass concentration in the batch studies. The data points represented at each CO_2 concentration are mean values of triplicate samples drawn from three repeated experiments (statistical significance; one way ANOVA; between the groups $p<0.005$ and r^2 0.98). (b) Goodness of fit plot showing the validation of experimental CO_2 transfer rate (Na(aq) with a theoretical mass transfer coefficient method; The data from both methods corelate establishing the accuracy of the CO_2 transfer rate from gas to liquid in the reactor. The data points represented at each CO_2 concentration are mean values of triplicate samples drawn from three repeated experiments (statistical significance; one way ANOVA; between the groups $p<0.005$ and r^2 0.98).

for various organisms.

Notable mass transfer methods, the CO_2 balance method of Eq. (3) and the CO_2 mass transfer coefficient method of Eq. (5), were used to determine the average CO_2 transferred in Nl culture. During gas-liquid mass transfer of CO_2 in the algal cultures, the amount of CO_2 transferred into the liquid culture is equivalent to the CO_2 concentration gradient created by an organism. The gradient is the transient demand by the organism equivalent to the volumetric uptake rate of CO_2 (Q_O). During the exponential phase of the algae, a steady state exists between CO_2 concentration gradient in the bulk liquid and the mass transfer of the CO_2 from gas to liquid. Thus, Q_O is indirectly quantified by measuring the mass transfer rate of CO_2 against the concentration gradient (Eq. (5)) using net molar aqueous CO_2 concentration with CO_2 mass balance method (Eq. (3)). Thus, the goodness of fit plot (Fig. 3(b)) validates the CO_2 transfer data with the Q_O at various CO_2 concentrations of the three microalgal species. The deviations of the data points on the line of fit are marginal ($p<0.005$, $r^2=0.98$) to contradict with the CO_2 transfer rate used in the calculation of E_{CO_2}. Therefore, the E_{CO_2} depicted in Table 3 supported with the validation of both CO_2 fixation data (Fig. 3(a), Fig. 3(b)) and the Q_O by indirectly measuring the CO_2 transfer rate with two independent methods (Fig. 3(b)). In conclusion, the E_{CO_2} was high (13.35%) at 3% CO_2 for Nl and 11.97% for Bb. In 10% CO_2, Nl could maintain marginally higher E_{CO_2} that was an average of 1.5 times higher than that of Bb and Sb.

2. Effect of CO_2 Enriched Air on Fatty Acid Profile

Elevated CO_2 concentration in the CO_2-enriched air had a considerable effect on the increase of mono-unsaturated fatty acid (MUFA) content (C18:1) of the alga from 13.2 to 36.2% with shift in CO_2 from 0.03-3%. Similarly, when the algae were exposed to 10% CO_2, the oleic acid was reduced to 32.4% as against 3% CO_2. The overall MUFA with oleic acid (Table 4) in particular increased, while the overall poly-unsaturated fatty acids (PUFA) reduced (11.4-6.7%) along with EPA (3.3-2.1%) with a shift in CO_2 from 3-10% in the Nl cultures. Tsuzuki et al. [36] and Dickson et al. [37] observed an increase in oleic acid content in *D. tertiolacta* and *Chlorella fusca* cultures with higher shifts in CO_2 concentration.

Table 4. Fatty acid composition of *N. limnetica* grown under various concentrations of CO_2 enriched air. The fatty acid percentage is depicted as mean values of three repeated experiments

Fatty acid	Fatty acid composition (%)		
	0.03% CO_2	3% CO_2	10% CO_2
16:0	24.7	17.6	23.0
16:1	36.9	34.2	36.8
17:1	0.8	0.6	1.1
18:1	13.2	36.2	32.4
18:2	5.4	3.6	1.4
18:3 (n-6)	0.7	1.1	0.7
20:4	5.8	3.4	2.5
20:5	12.5	3.3	2.1
ΣSFA	24.7	17.6	23.0
ΣMUFA	50.9	71.0	70.3
ΣPUFA	24.4	11.4	6.7
ΣTFA	100	100	100

SFA: Saturated fatty acids
MUFA: Monounsaturated fatty acids
PUFA: Poly un-saturated fatty acids
TFA: Total fatty acids

In the present work, the production of high oleic acid and low EPA at higher CO_2 concentrations could be considered as a possible mechanism of the algae to counteract the CO_2 stress induced by the high CO_2. The enzyme de-saturase, which requires oxygen, plays a key role in induction of multiple de-saturations in fatty acids. However, high CO_2 in the atmosphere is found to be a major limitation for impaired fatty acid conversion. Thus, EPA was inhibited, while MUFA synthesis was promoted.

Earlier studies [38,39] reveal that, under stressed conditions (nitrogen limitation, high-salinity, and light intensity), EPA concentration in species of *Nannochloropsis* was negatively affected. Chrismadha and Borowitzka [40] showed a decrease in EPA with an increase in CO_2 in *P. tricornatum*. In contrast, Hoshida et al. [22] showed a positive effect of CO_2 concentration (on-off mechanism of intermittent increase in CO_2 experiments) on EPA content. However, the operational CO_2 concentrations of 0.3% and 3% CO_2 used in their work were lower with an intermittent supply of CO_2. Hence, the effect could not be correlated with the present data. Moreover, it is well known that high oleic acid and low EPA are desirable for biofuel production. Moreover, the lower melting point of oleic acid and its oxidative stability also contribute towards enhancing biodiesel properties [41]. Therefore, *N. limnetica* grown under optimized operational conditions in CO_2-enriched air seems to be more suitable for biodiesel applications.

CONCLUSIONS

The biomass, lipid productivity, volumetric CO_2 uptake rate, and CO_2 capture efficiency of three algal species were studied. Overall, under CO_2-enriched environment, *Nannochloropsis limnetica* showed better performance over other cultures. Growing *N. limnetica* under elevated CO_2 for higher CO_2 capture along with an increase in oleic acid production and low EPA in its lipids is considered to be a better strategy in production of biomass feedstock for fuel applications.

ACKNOWLEDGEMENTS

This work was supported by the Department of Biotechnology, Ministry of Science and Technology, Government of India, New Delhi under the grant (Grant No. BT/PR11888/PBD/26/194/2009).

REFERENCES

1. B. Lee, G.-G. Choi, Y.-E. Choi, M. Sung, M. S. Park, J.-W. Yang, *Korean J. Chem. Eng.*, **31**, 1036 (2014).
2. T. Mutanda, D. Ramesh, S. Karthikeyan, S. Kumari, A. Anandraj and F. Bux, *Bioresour. Technol.*, **102**, 57 (2011).
3. S. R. Ronda, P. L. C. Parupudi, S. Vemula, S. Tumma, M. Botlagunta, V. S. Settaluri, S. Lele, S. Sharma and C. Kandala, *Korean J. Chem. Eng.*, **31**, 1839 (2014).

4. É. C. Francisco, D. B. Neves, E. Jacob-Lopes and T. T. Franco, *J. Chem. Technol. Biotechnol.*, **85**, 395 (2010).
5. L. Krienitz and M. Wirth, *Limnologica*, **36**, 204 (2006).
6. P. Cheng, B. Ji, L. Gao, W. Zhang, J. Wang and T. Liu, *Bioresour. Technol.*, **138**, 95 (2013).
7. G. Olivieri, A. Marzocchella, R. Andreozzi, G. Pinto and A. Pollio, *J. Chem. Technol. Biotechnol.*, **86**, 776 (2011).
8. J. Liu, J. Mukherjee, J. J. Hawkes and S. J. Wilkinson, *J. Chem. Technol. Biotechnol.*, **88**, 1807 (2013).
9. F. Mus, J. P. Toussaint, K. E. Cooksey, M. W. Fields, R. Gerlach, B. M. Peyton and R. P. Carlson, *Appl. Microbiol. Biotechnol.*, **97**, 3625 (2013).
10. C. Yoo, S. Y. Jun, J. Y. Lee, C. Y. Ahn and H. M. OH, *Bioresour. Technol.*, **101**, S71 (2010).
11. S. Y. Chiu, C. Y. Kao, M. T. Tsai, S. C. Ong, C. H. Chen and C. S. Lin, *Bioresour. Technol.*, **100**, 833 (2009).
12. G. Olivieri, I. Garganoa, R. Andreozzia, R. Marottaa, A. Marzocchellaa, G. Pintob and A. Polliob, *Chem. Eng. Trans.*, **27**, 127 (2012).
13. G. Olivieri, I. Gargano, R. Andreozzi, R. Marotta, A. Marzocchella, G. Pinto and A. Pollio, *Biochem. Eng. J.*, **74**, 8 (2013).
14. Y. T. Huang, H. T. Lee and C. W. Lai, *J. Nanosci. Nanotechnol.*, **13**, 2117 (2013).
15. S. Li, S. Luo and R. Guo, *Bioresour. Technol.*, **136**, 267 (2013).
16. A. Toledo-Cervantes, M. Morales, E. Novelo and S. Revah, *Bioresour. Technol.*, **130**, 652 (2013).
17. M. G. De Morais and J. A. V. Costa, *J. Biotechnol.*, **129**, 439 (2007).
18. A.Widjaja, C. C. Chien and Y. H. Ju, *J. Taiwan Inst. Chem. E.*, **40**, 13 (2009).
19. M. A. Islam, G. A. Ayoko, R. Brown, D. Stuart and K. Heimann, *Procedia. Eng.*, **56**, 591 (2013).
20. E. Y. Ortiz Montoya, A. A. Casazza, B. Aliakbarian, P. Perego, A. Converti and J. C. M. de Carvalho, *Biotechnol. Progr.*, **30**, 916 (2014).
21. Y. A. M. Yusof, J. M. H. Basari, N. A. Mukti, R. Sabuddin, A. R. Muda, S. Sulaiman, S. Makpol and W. Z. W. Ngah, *Afr. J. Biotechnol.*, **10**, 13536 (2013).
22. M. Tsuzuki, E. Ohnuma, N. Sato, T. Takaku, A and Kawaguchi, *Plant. Physiol.*, **93**, 851 (1990).
23. E. A. Muradyan, G. L. Klyachko-Gurvich, L. N. Tsoglin, T. V. Sergeyenko and N. A. Pronina, *Russ. J. Plant Physiol.*, **51**, 53 (2004).
24. H. Hoshida, T. Ohira, A. Minematsu, R. Akada and Y. Nishizawa, *J. Appl. Phycol.*, **17**, 29 (2005).
25. C. Largeau, E. Casadevall, C. Berkaloff and P. Dhamelincourt, *Phytochem.*, **19**, 1043 (1980).
26. Y. Shen and W. Q. Yuan, *Adv. Mater. Res.*, **393**, 655 (2012).
27. C. Zhu and Y. Lee, *J. Appl. Phycol.*, **9**, 189 (1997).
28. E. Ono and J. Cuello, *Biosystems Eng.*, **96**, 129 (2007).
29. J. Folch, M. Lees and G. Sloane-Stanley, *J. Biol. Chem.*, **226**, 497 (1957).
30. G. Lepage and C. C. Roy, *J. Lipid Res.*, **25**, 1391 (1984).
31. T. L. Bergman, F. P. Incropera, A. S. Lavine and D. P. DeWitt, *Fundamentals of heat and mass transfer*, Seventh Ed., John Wiley and Sons, New York (2011).
32. Y. Ge, J. Liu and G. Tian, *Bioresour. Technol.*, **102**, 130 (2011).
33. C. Dayananda, R. Sarada, M. Usha Rani, T. Shamala and G. Ravishankar, *Biomass Bioenerg.*, **31**, 87 (2007).
34. L. Krienitz, D. Hepperle, H. B. Stich and W. Weiler, *Phycologia*, **39**, 19 (2000).
35. D. Tang, W. Han, P. Li , X. Miao and J. Zhong, *Bioresour. Technol.*, **102**, 3071 (2011).
36. M. Tsuzuki, M. Gantar, K. Aizawa and S. Miyachi, *Plant Cell Physiol.*, **27**, 737 (1986).
37. L. G. Dickson, R. A. Galloway and G. W. Patterson, *Plant. Physiol.*, **44**, 1413 (1969).
38. M. Hoffmann, K. Marxen, R. Schulz and K. H. Vanselow, *Mar. Drugs*, **8**, 2526 (2010).
39. D. Pal, I. Khozin-Goldberg, Z. Cohen and S. Boussiba, *Appl. Microbiol. Biotechnol.*, **90**, 1429 (2011).
40. T. Chrismadha and M. A. Borowitzka, *J. Appl. Phycol.*, **6**, 67 (1994).
41. G. Knothe, *Energy Fuels*, **22**, 1358 (2008).